

Research Article

Open Access



# *In situ* study of phase transition in HZO ferroelectric thin films via TEM electron beam irradiation

Ke Cao<sup>1,2,#</sup>, Quanlin Zhao<sup>1,#</sup>, Jiajia Liao<sup>1,2</sup>, Fei Yan<sup>1,2</sup>, Keyu Bao<sup>1</sup>, Shijie Jia<sup>1</sup>, Jianquan Zhang<sup>1</sup>, Junhui Luo<sup>1</sup>, Min Liao<sup>1,2</sup>, Yichun Zhou<sup>1,2</sup>

<sup>1</sup>School of Advanced Materials and Nanotechnology, Xidian University, Xi'an 710126, Shaanxi, China.

<sup>2</sup>Shaanxi Key Laboratory of High-Orbits-Electron Materials and Protection Technology for Aerospace, Xidian University, Xi'an 710126, Shaanxi, China.

#Authors contributed equally.

**Correspondence to:** Prof. Fei Yan, School of Advanced Materials and Nanotechnology, Xidian University, 266 Xinglong Section of Xifeng Road, Xi'an 710126, Shaanxi, China. E-mail: yanfei@xidian.edu.cn; Prof. Yichun Zhou, School of Advanced Materials and Nanotechnology, Xidian University, 266 Xinglong Section of Xifeng Road, Xi'an 710126, Shaanxi, China. E-mail: yichunzhou@xidian.edu.cn

**How to cite this article:** Cao, K.; Zhao, Q.; Liao, J.; Yan, F.; Bao, K.; Jia, S.; Zhang, J.; Luo, J.; Liao, M.; Zhou, Y. *In situ* study of phase transition in HZO ferroelectric thin films via TEM electron beam irradiation. *Microstructures* 2025, 5, 2025025. <https://dx.doi.org/10.20517/microstructures.2024.120>

**Received:** 13 Nov 2024 **First Decision:** 13 Jan 2025 **Revised:** 11 Feb 2025 **Accepted:** 21 Feb 2025 **Published:** 14 Mar 2025

**Academic Editor:** Shujun Zhang **Copy Editor:** Fangling Lan **Production Editor:** Fangling Lan

## Abstract

Oxygen vacancies ( $V_o$ ) play a crucial role in the stability of the ferroelectric orthorhombic (o-) phase of hafnium dioxide ( $HfO_2$ )-based thin films. However, the stability of the ferroelectric phase of  $HfO_2$  under the action of  $V_o$  and the mechanism of ferroelectric phase transition are still unclear. In this work,  $V_o$  concentration in  $Hf_{0.5}Zr_{0.5}O_2$  (HZO) thin films is tuned through electron beam irradiation inside a transmission electron microscope. For the crystalline HZO thin films processed through rapid thermal annealing, the increase of the  $V_o$  concentration during *in situ* electron beam irradiation facilitated the phase transition from the non-polar monoclinic (m-) and tetragonal (t-) phases to the polar o-phase. For the amorphous HZO thin films, the nucleation and growth process of the m- and o-phases are observed during *in situ* electron beam irradiation. The phase transition from m-phase to o-phase is accompanied by the evolution from tensile to compressive strain. These results help to clarify the mechanism of ferroelectric phase transition under the action of  $V_o$ , and guide the control of the ferroelectric properties and phase stability of  $HfO_2$ -based thin films.

**Keywords:** Ferroelectric film,  $Hf_{0.5}Zr_{0.5}O_2$ , oxygen vacancy, phase transition, electron beam irradiation



© The Author(s) 2025. **Open Access** This article is licensed under a Creative Commons Attribution 4.0 International License (<https://creativecommons.org/licenses/by/4.0/>), which permits unrestricted use, sharing, adaptation, distribution and reproduction in any medium or format, for any purpose, even commercially, as long as you give appropriate credit to the original author(s) and the source, provide a link to the Creative Commons license, and indicate if changes were made.



## INTRODUCTION

Ferroelectric materials have great potential in electronic information technology, especially in ferroelectric storage and computing devices, such as ferroelectric field-effect transistors and nonvolatile memories<sup>[1,2]</sup>. However, traditional perovskite-structured ferroelectric thin film materials suffer from poor compatibility with complementary metal-oxide-semiconductor (CMOS) technology, limited miniaturization, low storage density, and environmental issues such as lead pollution<sup>[3]</sup>. In contrast, hafnium dioxide (HfO<sub>2</sub>)-based ferroelectrics offer a promising alternative due to their excellent CMOS compatibility, wide bandgap, high storage density, low energy consumption, and scalability to nanoscale dimensions<sup>[4,5]</sup>. The ferroelectricity of HfO<sub>2</sub> was first discovered in 2011 in Si-doped HfO<sub>2</sub> thin films<sup>[6]</sup>, a breakthrough that has since spurred widespread interest in both ferroelectric materials and memory devices<sup>[7]</sup>. Subsequent research has shown that the ferroelectricity of HfO<sub>2</sub>-based thin films originates from the non-centrosymmetric Pca2<sub>1</sub> ferroelectric o-phase<sup>[8]</sup>. Recent studies have further demonstrated the immense potential of HfO<sub>2</sub>-based systems: for instance, atomic-scale ferroelectric tunnel junctions with unprecedented scaling have been reported<sup>[9]</sup>, and record-high 300 K-resistance switching in ferroelectric-gated Mott transistors has been achieved<sup>[10]</sup>. However, multiphase, including orthorhombic, monoclinic (m-), and tetragonal (t-) phases, coexist in the atomic layer deposition (ALD)-fabricated HfO<sub>2</sub>-based thin films due to the metastable characteristic of the o-phase<sup>[11-13]</sup>. Therefore, controlling and stabilizing the ferroelectric o-phase is critical to achieving superior device performance of HfO<sub>2</sub>-based thin films<sup>[14]</sup>.

Oxygen vacancies (V<sub>O</sub>) are an important factor affecting the stability of the HfO<sub>2</sub> o-phase; thus, the ferroelectricity of HfO<sub>2</sub> can be regulated by tuning the V<sub>O</sub><sup>[15,16]</sup>. First-principles density functional theory (DFT) calculations confirmed that increasing the concentration of V<sub>O</sub> within a certain range is beneficial to the stability of the o-phase because the presence of V<sub>O</sub> promotes the generation of the o-phase<sup>[17]</sup>. Furthermore, V<sub>O</sub> in HfO<sub>2</sub> can exist in several charge states. Most first-principles studies typically consider at least three major charge states: the neutral vacancy (V<sub>O</sub><sup>0</sup>), the singly positively charged vacancy (V<sub>O</sub><sup>+</sup>), and the doubly positively charged vacancy (V<sub>O</sub><sup>2+</sup>). In many cases - especially in the context of ferroelectric phase stabilization - the doubly charged state (V<sub>O</sub><sup>2+</sup>) has been highlighted as particularly significant because its formation and lower diffusion barrier help to promote the phase transition from the non-polar to the ferroelectric state<sup>[16,18]</sup>. V<sub>O</sub> can be introduced into HfO<sub>2</sub> by optimizing deposition conditions such as O reactant species and deposition temperature, and doping of bi- or tri-valent chemical species to meet the charge neutrality condition, *etc.*<sup>[19-21]</sup>. The concentration of V<sub>O</sub> in ALD-fabricated HfO<sub>2</sub>-based ferroelectric thin films could be reduced by oxygen plasma (O<sub>2</sub> Plasma) treatment or O<sub>3</sub> treatment, macroscopically manifested as decay of ferroelectric performance<sup>[22]</sup>. The decrease in V<sub>O</sub> concentration changes the stability of each phase in the film, which reduces the content of the o-phase evidenced by phase composition characterization experiments<sup>[15,23]</sup>. It was found that *in situ* irradiation of Hf<sub>0.5</sub>Zr<sub>0.5</sub>O<sub>2</sub> (HZO) ferroelectric thin films with an electron beam can induce the generation and redistribution of V<sub>O</sub>, causing local stress fields, thereby affecting the stability and migration of 90° ferroelectric domain walls<sup>[24]</sup>. At the same time, the local stress field caused by the generation and redistribution of V<sub>O</sub> plays an important role in the ferroelectric phase transition. Up to now, the results of theoretical calculations and experiments of V<sub>O</sub> or strain effects on the stability of o-phase are not consistent. In DFT calculations, it is believed that in-plane compressive stress is beneficial for the stability of the o-phase, while in-plane tensile stress significantly promotes the stability of the m-phase<sup>[25-27]</sup>. However, in experiments, by applying different stresses to the HfO<sub>2</sub>-based thin film through different element doping, different thermal expansion coefficient electrode materials, different electrode sizes, and different substrates, it was found that in-plane tensile stress is beneficial for the stability of the o-phase, but not for the stability of the m-phase<sup>[6,28,29]</sup>.

In this work, the high-energy electron beam of a transmission electron microscope (TEM) was used to tune the  $V_O$  in HZO ferroelectric thin films, and to reveal the effect of  $V_O$  concentration on the ferroelectric phase transition of HZO thin films and unveil its ferroelectric phase transition mechanism. It was found that the concentration of  $V_O$  in the HZO ferroelectric thin film significantly increased after electron beam irradiation, accompanied by a phase transition from the m-phase to the o-phase. Meanwhile, geometric phase analysis (GPA) found that during the phase transition of HZO ferroelectric thin films from m-phase to o-phase, the state of strain changes, gradually transitioning from tensile strain to compressive strain. Similarly, we observed the phase transition process from the t-phase to the o-phase, as well as the nucleation and growth of the m-phase and the o-phase under electron beam irradiation in amorphous HZO thin films. These results help to reveal the phase transition mechanism of  $HfO_2$ -based ferroelectric thin films assisted with  $V_O$ , guiding the phase stability and ferroelectric performance optimization of  $HfO_2$ -based ferroelectric thin films.

## MATERIALS AND METHODS

### HZO ferroelectric capacitors and cross-sectional TEM sample preparation

#### *Fabrication of MFM structure HZO ferroelectric capacitors*

For the preparation of the HZO ferroelectric capacitor for ferroelectric performance testing and phase structure characterization, first, a W/TiN bottom electrode with a thickness of about 40 nm was deposited on a heavily doped P-type silicon substrate using magnetron sputtering. Next, with  $Hf[N(CH_3)_2]_4$  (Tetrakis dimethylamido hafnium, TDMAHf) and  $Zr[N(CH_3)_2]_4$  (Tetrakis dimethylamino zirconium, TDMAZr) as precursors and deionized water as the oxygen source, an HZO thin film with a thickness of about 14 nm was deposited on the W/TiN bottom electrode using ALD (Savannah G2 s200, Ultratech/CNT™) at a deposition chamber temperature of 270 °C and a cycle ratio of Hf precursor to Zr precursor of 1:1. Subsequently, a W/TiN top block electrode or dot electrode with a thickness of about 15 nm was deposited directly or by adding a mask using magnetron sputtering. Finally, the prepared HZO capacitor was rapidly thermally annealed (RTP-150-EP, UniTemp™) at 550 °C for 30 s for crystallization.

#### *HZO ferroelectric film TEM sample preparation*

A focused ion beam system (Helios 5 CX, Thermo Fisher Scientific™) was used to prepare cross-sectional samples of HZO ferroelectric capacitors for characterization by TEM. First, a layer of platinum (Pt) was deposited at the top electrode of the HZO ferroelectric capacitor to protect thin films. Next, a lamella of HZO ferroelectric capacitor sample with dimensions of 10  $\mu\text{m}$   $\times$  2  $\mu\text{m}$   $\times$  8  $\mu\text{m}$  (length  $\times$  width  $\times$  height) was cut and lifted out, and welded onto a standard half-copper grid. Finally, the lamella was gradually thinned to a thickness of about 50 nm with decreasing accelerating voltage and Ga ion beam current, thus preparing a cross-sectional sample of HZO ferroelectric thin film for *in situ* TEM electron beam irradiation.

### Structure characterization and ferroelectric performance testing of the fabricated HZO ferroelectric film

The phase composition of the W/HZO/W ferroelectric capacitor was characterized using a grazing incidence X-ray diffractometer (Smartlab 9 kW, Rigaku™). The grazing incidence angle was 0.5°, the scan step was 0.002°, and the scan range was 2 $\theta$  from 25° to 55°.

The HZO ferroelectric thin film was tested for dynamic hysteresis [polarization-voltage ( $P$ - $V$ )] using a ferroelectric analyzer (axiACTT TF analyzer 3000, Germany).  $P$ - $V$  curve test conditions: 1 kHz triangular wave, 4 V pulse voltage. Wake-up conditions: 100 Hz square wave, 3.5 V pulse voltage, 1,000 cycles.

## HZO ferroelectric film TEM microstructure characterization and in situ electron beam irradiation

A TEM (FEI Talos F200X, Thermo Fisher Scientific™) was used for TEM characterization of the cross-sectional samples of the HZO ferroelectric thin film and electron beam irradiation with an accelerating voltage of 200 keV. The electron beam spot diameter was scaled down to about 20 nm for continuous irradiation of the HZO thin film. At this time, the electron beam current density was approximately 40,000 e/Å<sup>2</sup> s, and HRTEM images were obtained every 3 min during irradiation. Elemental dispersive X-ray spectroscopy (EDX) elemental distribution characterization was performed on the same area of the HZO thin film before and after electron beam irradiation. The relative ratio (atomic ratio) of Hf atoms to O atoms along the growth direction of the HZO thin film was chosen as the evaluation standard for semi-quantitatively analyzing the V<sub>o</sub> concentration in the thin film.

## RESULTS AND DISCUSSION

### Characterization of ALD fabricated HZO thin films

The HZO ferroelectric films with Metal-Ferroelectric-Metal (MFM) structures were fabricated through an ALD method as shown in [Figure 1A](#). The specific fabrication process is described in the Section “MATERIALS AND METHODS”. [Figure 1B](#) displays the cell structure models of the centrosymmetric t-phase and the o-phase of the HZO thin film, showing that the two structures are very similar. In this figure, the solid orange-yellow spheres represent hafnium (Hf) or zirconium (Zr) ions. In the t-phase, all oxygen ions are located at the center of the nearest Hf/Zr ions, represented by gray solid spheres, as four-coordinated oxygen ions. However, in the o-phase, in addition to the tetra-coordinated oxygen ions located at the center position of the nearest Hf/Zr ions, there are non-centrosymmetric triple-coordinated oxygen ions offset along the c-axis direction, represented by red solid spheres. This is widely believed to be the origin of the ferroelectricity in HfO<sub>2</sub>-based thin films<sup>[30]</sup>. To determine the composition of the fabricated HZO ferroelectric thin film, [Figure 1C](#) presents the results of the grazing incidence X-ray diffraction (GIXRD) tests conducted at a grazing incidence angle of 0.5°. The main phase of the thin film is the o-phase/t-phase, with a prominent peak at approximately 30.5°, corresponding to O(111)/T(101), and a weaker peak near 28.3°, corresponding to M( $\bar{1}$ 11). This reveals that the thin film primarily consists of the o-phase and the t-phase. The structures of the o- and the t-phase are similar, resulting in their diffraction peaks at 30.5° being very close, making it hard to distinguish them through GIXRD<sup>[31]</sup>. Meanwhile, the *P-V* hysteresis loop and the current (*I*)-*V* curve were shown in [Figure 1D](#) with a 1 kHz and 4 V pulse voltage. The wake-up was tested with 100 Hz, 3.5 V pulse voltage at 1,000 cycles. The prepared HZO ferroelectric thin film showed good ferroelectric performance. After being awakened, the residual polarization value *P<sub>r</sub>* was 22.9 μC/cm<sup>2</sup> under the test voltage of 4 V. At the same time, its polarization switching current peak was visible, and there was no leakage current under this voltage.

### Electron beam-induced V<sub>o</sub> in HZO films inside TEM

The cross-sectional view of the fabricated HZO film is shown in [Figure 2A](#). The polycrystal HZO layer with a thickness of 14 nm was sandwiched between two W layers (top layer around 15 nm), as shown in the high-resolution TEM (HRTEM) image in [Figure 2A](#). The interfaces between the HZO thin film and the top and bottom electrodes were smooth. *In situ* electron beam irradiation was carried out inside TEM on the fabricated ferroelectric film as illustrated in [Figure 2B](#), and the V<sub>o</sub> concentration was analyzed during electron beam irradiation through EDX. By adjusting the diameter of the electron beam, the dosage of the electrons bombarded on the sample area was tuned, and HRTEM images during the irradiation process were captured every minute.

A semi-quantitative analysis of the V<sub>o</sub> concentration changes in the HZO ferroelectric thin film before and after electron beam irradiation was performed using EDX analysis, with the results presented in [Figure 2C](#). The relative ratio (relative fraction) of Hf to O atoms was selected as the function for the vertical axis

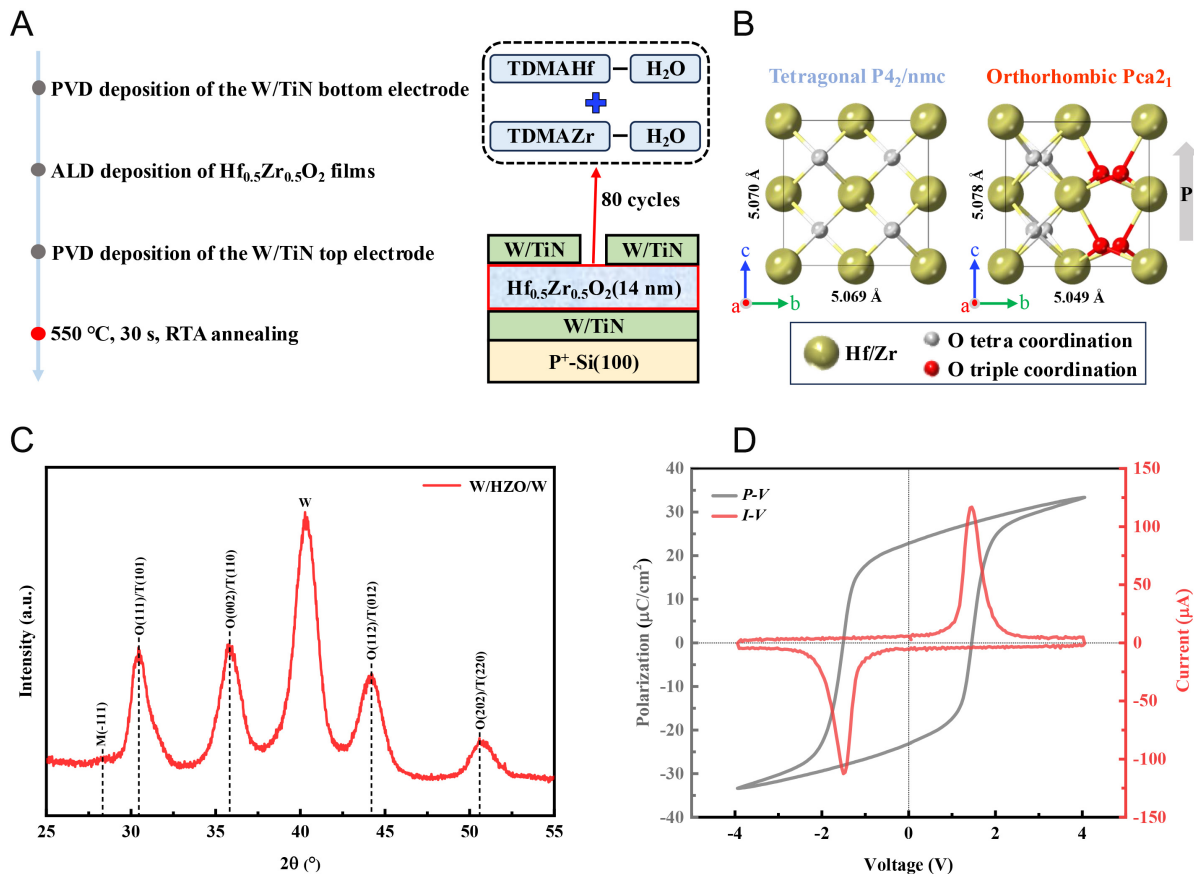


**Figure 1.** (A) Fabrication process of HZO ferroelectric capacitor, (B) Structural models of a non-polar t-phase with space group  $P4_2/nmc$  and a polar o-phase with space group  $Pca2_1$ , (C) GI-XRD pattern of W/HZO/W ferroelectric thin film, (D)  $P-V$  and  $I-V$  curves of HZO ferroelectric thin film.

coordinates. A higher relative fraction indicates a higher concentration of  $V_{\text{O}}$ . The intensity ratio of Hf and O in the red line after irradiation was increased than before in the black line within the HZO layer denoted with green color; thus, the  $V_{\text{O}}$  in the HZO thin film was increased after an hour of electron beam irradiation, especially in the region near the top electrode layer. This may be attributed to the asymmetry fabrication process of the ferroelectric capacitor. The Knotek-Feibelman mechanism for radiolysis is suggested as the mechanism of the introduction of  $V_{\text{O}}$ . First, the electron beam creates an inner-shell vacancy on the metal site. Next, an electron from a nearby oxygen atom has an interatomic Auger decay to the metal inner shell hole, and further Auger electrons are ejected from the oxygen atom. This results in a neutral or positive oxygen atom that is repelled by the surrounding metal ions and ejected into the vacuum<sup>[32,33]</sup>. The  $V_{\text{O}}$  concentration induced by electron beam irradiation depends on irradiation parameters such as electron beam energy, dose rate, exposure time, *etc.* Under controlled conditions, the  $V_{\text{O}}$  concentration remains relatively stable during experiments. A moderate concentration of vacancies lowers the switching barrier and enhances polarization, whereas excessive vacancy formation can lead to defect clustering, increased leakage, and domain wall pinning<sup>[2,19,22]</sup>. To exclude the influence of the material of the electrode layer, the W/HZO/W ferroelectric capacitor was also fabricated and irradiated; the EDX results were shown in [Supplementary Figure 1](#), which demonstrated a similar increasing trend of  $V_{\text{O}}$ . These results confirmed that electron beam irradiation can lead to the increase of the  $V_{\text{O}}$  in the sample.

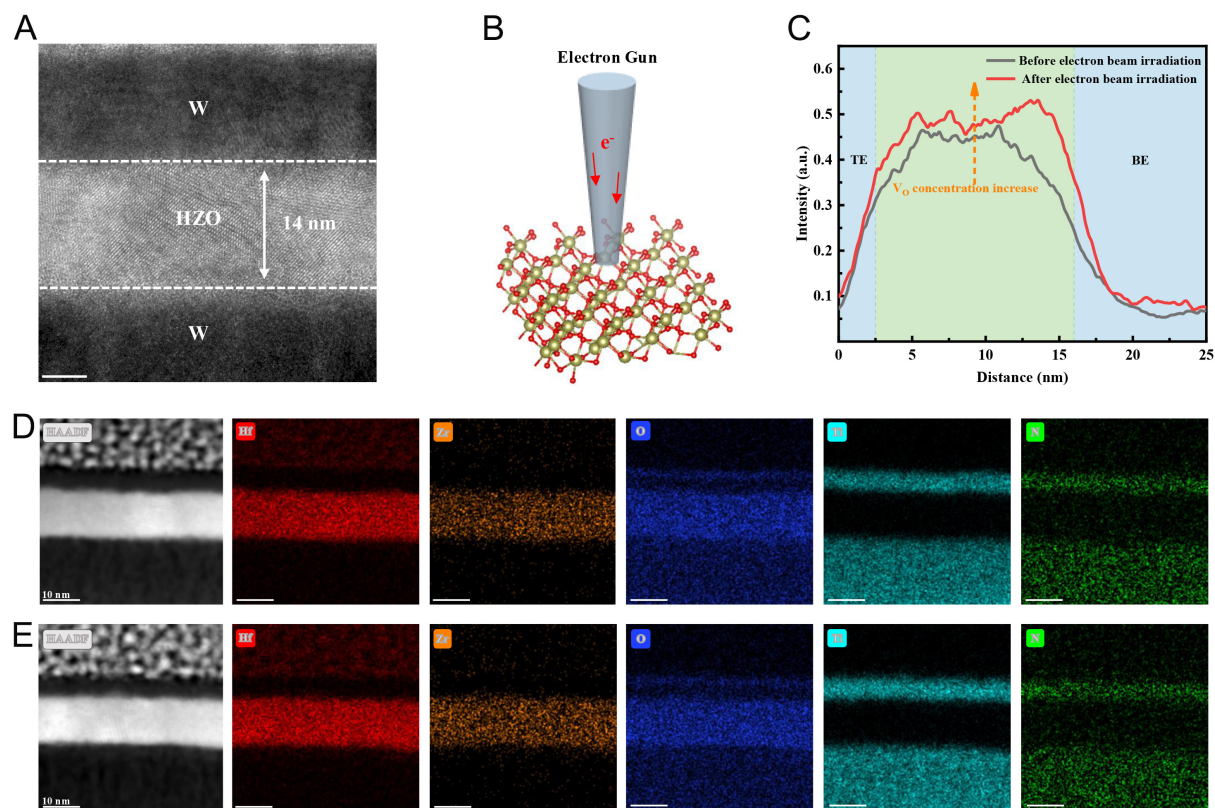


**Figure 2.** (A) HRTEM image of the cross-sectional morphology of the HZO ferroelectric capacitor, (B) Schematic diagram of electron beam irradiation, scale bar 5 nm, (C) Semi-quantitative analysis of  $V_O$  concentration before and after electron beam irradiation of the TiN/HZO/TiN ferroelectric thin film, (D) EDX element mapping of the TiN/HZO/TiN ferroelectric thin film before electron beam irradiation, scale bar 10 nm, (E) EDX element mapping of the TiN/HZO/TiN ferroelectric thin film after electron beam irradiation, scale bar 10 nm.

The element distribution along the growth direction of the HZO thin film was characterized with line-profile EDX analysis<sup>[31]</sup>. Before irradiation, as shown in Figure 2D, the high-angle annular dark field (HAADF) image demonstrated the sample area before exposure, with Hf, Zr, and O elements distributed evenly in the middle layer. Titanium (Ti) and nitrogen (N) were distributed in the top and bottom electrode layers. The diffusion of elements across different layers was not obvious. In Figure 2E, the elements showed diffusion across different layers which may be attributed to the joule heating phenomenon of the electron beam irradiation<sup>[34]</sup>. The joule heating phenomenon caused the local temperature rise in the irradiated area, thus leading to the diffusion of the elements.

### Ferroelectric phase transition in HZO thin films by electron beam irradiation

Electron beam irradiation-induced phase transition from m-phase to o-phase was observed inside TEM. The focused-ion-beam (FIB) thinned cross-sectional HZO ferroelectric film was irradiated with Talos F200X TEM, under 200 kV accelerating voltage. The irradiated area of the HZO thin film was confined to a circular region with a diameter of about 20 nm, and the electron beam current density was about  $410^4 e/(\text{\AA}^2 \text{s})$ . The HRTEM image was captured every 3 min, as shown in Figure 3. The pristine HZO ferroelectric film was a m-phase in the red rectangle area of Figure 3A. The area was the o-phase after being irradiated for 30 min under the electron beam denoted with a green rectangle in Figure 3D. The irradiated area underwent phase transition from m-phase with zone axis  $[1\bar{1}0]$  to po phase with zone axis  $[010]$ , which was identified in the fast Fourier transformation (FFT) image. The increased  $V_O$  concentration during the

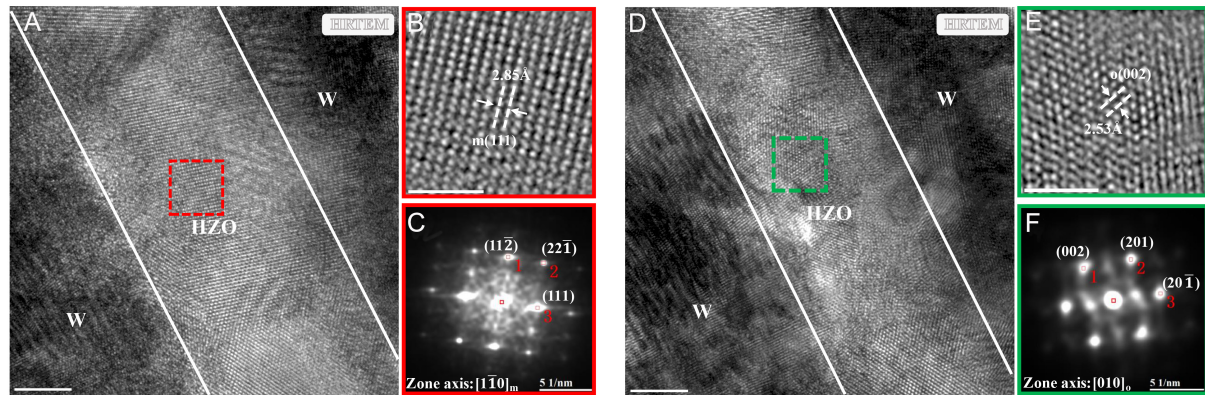


**Figure 3.** (A) HRTEM image of the HZO ferroelectric thin film before electron beam irradiation, scale bar 5 nm. (B) Magnified image of the m-phase in the red box area, scale bar 2 nm. (C) FFT image of the red box area, (D) HRTEM image of the HZO ferroelectric thin film after electron beam irradiation, scale bar 5 nm. (E) Magnified image of the o-phase in the green box area, scale bar 2 nm. (F) FFT image of the green box area.

irradiation process contributes to the phase transition; this has been confirmed in previous research such as O vacancy engineering, helium (He) ion irradiation-induced phase transformation, and ferroelectric transition under biasing voltage, all of which proved the  $V_O$  are beneficial to the phase transition<sup>[2,35,36]</sup>. From the above EDX results in Figure 2, the  $V_O$  concentration increased after the electron beam irradiation for 60 min. The high energy electrons collided with O atoms and left with  $V_O$  in the original location. The charged  $V_O$  in the pristine m-phase increases, thereby lowering the phase transition potential barrier from the m-phase to the o-phase, which was proved from DFT in previous research<sup>[37]</sup>. As the electron beam irradiation continues, the m-phase absorbs the energy of the energetic electrons and converts it into its internal energy. Thus, at some critical point, the phase transition potential barrier from the m-phase to the o-phase is crossed and the phase transition is finally completed.

Similarly, the phase transition from the t-phase to the o-phase was also observed through *in situ* electron beam irradiation experiments on HZO thin films, as shown in Supplementary Figure 2. The ferroelectric phase transition occurred just 90 s after irradiation, indicating that compared to the phase transition from the m-phase to the o-phase, the phase transition from the t-phase to the o-phase requires a smaller transition barrier, which is consistent with previous research because increase in the concentration of the  $V_O$  lowers its phase transition barrier<sup>[37,38]</sup>. In addition, this type of phase transition has also been widely observed in related studies of thermal fields<sup>[39]</sup>, wake-up<sup>[40]</sup>, and strain engineering<sup>[41]</sup>. The wake-up effect is characterized by an increase in remnant polarization ( $P_r$ ) after a number of electric field cycles, which may be attributed to the redistribution of  $V_O$  and field-driven phase transformation from t-phase to o-phase during electric field cycling<sup>[42]</sup>. In addition, some reports also pointed out that the wake-up effect is related to the suppression of disorder<sup>[11]</sup>. Herein, we are focused on investigating the  $V_O$  concentration and phase transition of HZO thin films during *in situ* TEM electron beam irradiation. In this process, it is difficult to observe the suppression of disorder. When irradiated for 690 s, a crystal zone axis flip occurred, from  $[1\bar{2}\bar{1}]_o$  to  $[001]_o$ , at which point the irradiated area presented an in-plane polarization state, as shown in Supplementary Figure 2C. Continuing irradiation, a crystal zone axis flip occurred, and the in-plane domain changed to an out-of-plane domain, i.e.,  $[100]_o$  and  $[010]_o$ , as shown in Supplementary Figure 2D and E. This behavior is one of the mechanisms of the wake-up effect of  $HfO_2$ -based ferroelectric thin films<sup>[43]</sup>; hence, this result provides new experimental evidence and control methods for the explanation of the wake-up effect mechanism of  $HfO_2$ -based ferroelectric thin films.

### Strain analysis of ferroelectric phase transition processes

During the phase transition of the  $\text{HfO}_2$ -based thin films, the strain distribution in the film was analyzed by the GPA method. Figure 4 shows the strain distribution during the phase transition of m-phase to o-phase. The obtained  $\varepsilon_{xx}$  and  $\varepsilon_{yy}$  images correspond to the stress distribution along the x-direction (i.e., the horizontal axis) of the analyzed region, and the strain in the y-direction, respectively (as shown in the FFT images of Figure 3C). It can be seen that there is almost no strain along the x-direction in the red box area, while there is a tensile strain on the y-direction, which can be seen in the yellow box area. The stress state of the m-phase within the red box area in Figure 4A at 0 min of electron beam irradiation is used as a reference. Upon the start of electron beam irradiation, the strain state change in the  $\varepsilon_{yy}$  image is substantial. After irradiation for 31 min [Figure 4E], a phase transition occurs; the crystal plane changes from  $m(11\bar{2})$  to  $o(002)$ , causing the yellow box area to change from tensile strain to compressive strain. As the irradiation time continues to increase, the compressive strain state in the red box area becomes more pronounced as shown in Figure 4F and G.

Moreover, the area of the unit cell projection plane corresponding to the  $[1\bar{1}0]m$  and  $[010]o$  crystal orientations was calculated before and after the phase transition. The cell parameters were obtained from the optimization calculation results of the DFT<sup>[44]</sup>. The cell parameters of the m-phase area = 5.33 Å,  $b = 5.20$  Å,  $c = 5.15$  Å,  $\alpha = 90^\circ$ ,  $\beta = 90^\circ$ ,  $\gamma = 99.7^\circ$ , and the cell parameters of the o-phase area = 5.27 Å,  $b = 5.05$  Å,  $c = 5.08$  Å,  $\alpha = 90^\circ$ ,  $\beta = 90^\circ$ ,  $\gamma = 90^\circ$ . The area of the unit cell projection plane corresponding to the  $[1\bar{1}0]m$  crystal orientation is  $S_m = 37.80$  Å<sup>2</sup>, and the area of the unit cell projection plane corresponding to the  $[010]o$  crystal orientation is  $S_o = 26.77$  Å<sup>2</sup> (as illustrated in Supplementary Figures 3 and 4). The calculation results show that the area of the unit cell projection plane corresponding to the  $[010]o$  crystal orientation after the phase transition is smaller than that corresponding to the  $[1\bar{1}0]m$  crystal orientation before the phase transition. This also confirms that there exists compressive strain during the phase transition process from the parent phase  $[1\bar{1}0]m$  to the new phase  $[010]o$ , consistent with the GPA results.

### Ferroelectric crystallization induced by electron beam irradiation of amorphous HZO thin films

During the semi-quantitative analysis of  $V_o$  concentration of HZO ferroelectric films before and after e-beam irradiation in Figure 2, it was found that electron beam irradiation was able to induce crystallization of amorphous HZO films, which is the electron beam heating effect, producing an effect similar to rapid thermal annealing (RTA)<sup>[45]</sup>. For the HZO thin film without RTA, its crystallinity was analyzed using GIXRD testing, with specific results shown in Supplementary Figure 5. Compared with the HZO ferroelectric thin film after RTA, it was determined that the HZO film without RTA exhibits strong amorphous characteristics. Therefore, the crystallization process of the HZO film under electron beam irradiation through *in situ* HRTEM is shown in Figure 5. First, after 10 s of high-energy electron beam irradiation, two nuclei begin to appear in the smooth and uniform amorphous HZO film in Figure 5A, being the ferroelectric o-phase and disordered polycrystalline, respectively. The nuclei continued to grow with prolonged irradiation accompanied by the formation and fusion of new nuclei in Figure 5B and C. Multiple o-phases and m-phases were observed in the HZO sample area. As the irradiation time increased to about 100 s in Figure 5D, the amorphous HZO area completely crystallized, and the phase transition to the o-phase and the m-phase occurred, which is similar to the phenomenon in RTA<sup>[46]</sup>. When the irradiation time was further extended to 110 s (see Figure 5E), the two o-phase grains experienced mutual squeezing. This interaction led to the generation of dislocations at the grain boundaries, as indicated by the purple box in Figure 5E. These dislocations may cause  $V_o$  to accumulate at these locations, which can subsequently lead to breakdown fatigue in the HZO ferroelectric film<sup>[47]</sup>. Until 200 s of irradiation, a part of the ferroelectric o-phase grains near the dislocations underwent a crystal zone axis flip. The interplanar spacing decreased from 3.033 to 1.515 Å, corresponding to the crystal plane changing from  $o(111)$  to  $o(131)$ , driven by the thermal effect of electron beam irradiation.

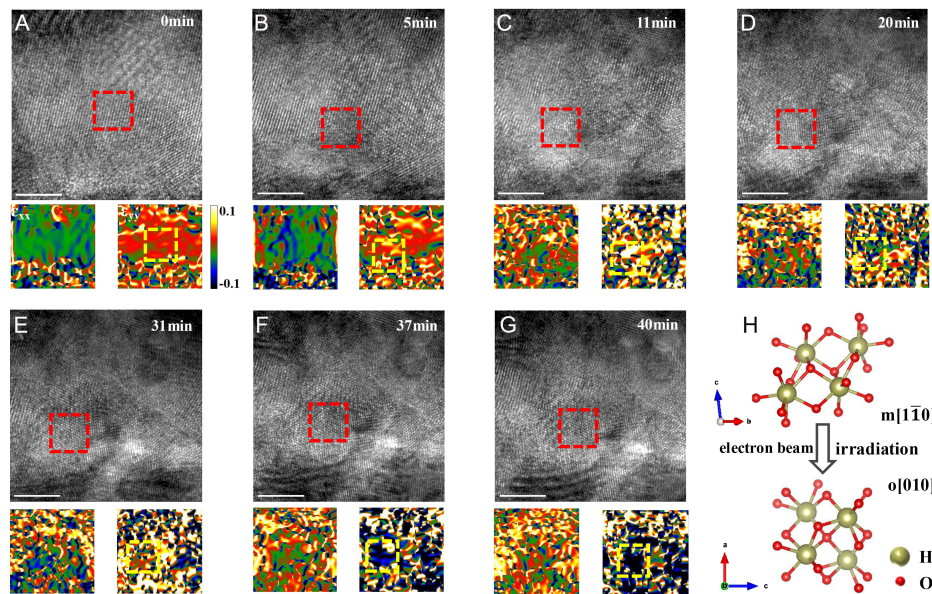


**Figure 4.** (A-G) HRTEM images of the HZO ferroelectric thin film during electron beam irradiation and the GPA analysis results of the corresponding red box area, scale bar 5 nm. (H) Schematic diagram of electron beam irradiation-induced ferroelectric phase transition in HZO thin film.

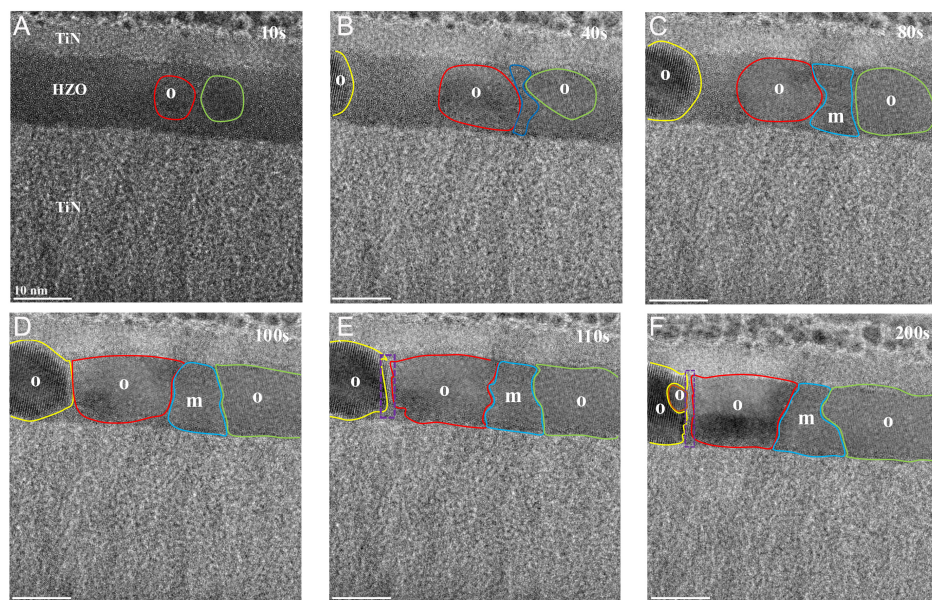


**Figure 5.** Electron beam irradiation-induced crystallization of amorphous HZO thin film: (A) nucleation begins in the o-phase, (B) growth of the o-phase nucleus, (C) growth of the nucleus in both the o-phase and m-phase, (D) complete crystallization of the amorphous HZO thin film, (E) generation of lattice dislocations at the interface, (F) rotation of the o-phase crystal axis. The scale bars are all 10 nm.

## CONCLUSIONS

In this work, the concentration of  $V_O$  in the HZO thin film was modified by *in situ* TEM electron beam irradiation, and the phase transition of the HZO thin film from the m-phase to the o-phase was demonstrated. The  $V_O$  in the thin film played a key role in this process, reducing the phase transition barrier from the m-phase to the o-phase. The phase transition process was accompanied by a change in the stress state, gradually shifting from tensile strain to compressive strain, and aligning with the phase transition critical point. Besides, *in situ* electron beam irradiation of the amorphous HZO thin film revealed that the effect of electron beam irradiation was similar to the thermal annealing process, causing the HZO thin film to grow from a disordered amorphous state into an ordered structure of the ferroelectric o-phase and m-phase. In conclusion, the above results reveal the mechanism of the ferroelectric phase transition of the HZO thin film with the influence of  $V_O$  and provide a new strategy for the optimization of the ferroelectric properties of  $HfO_2$ -based thin films.

## DECLARATIONS

### Authors' contributions

Made substantial contributions to conception and design of the study and performed data analysis and interpretation: Cao, K.; Zhao, Q.; Liao, J.; Yan, F.; Liao, M.; Zhou, Y.

Performed data acquisition and provided administrative, technical, and material support: Bao, K.; Jia, S.; Zhang, J.; Luo, J.

### Availability of data and materials

All data needed to support the conclusions in the paper are presented in the manuscript and/or the [Supplementary Material](#). Additional data related to this paper may be requested from the corresponding author upon request.

### Financial support and sponsorship

This work is granted by the National Natural Science Foundation of China (Nos. 12202330, 52302151, 12302429, 11932016), the open foundation of Hubei Key Laboratory of Theory and Application of Advanced Materials Mechanics (Wuhan University of Technology) (No. TAM202204), Qin Chuang Yuan Cited High-level Innovation and Entrepreneurship Talent Project (Grant No. QCYRCXM-2023-075), Fundamental Research Funds for the Central Universities (Grant No. ZYTS24122), and the Guangdong Basic and Applied Basic Research Foundation (2022A1515110116).

### Conflicts of interest

All authors declared that there are no conflicts of interest.

### Ethical approval and consent to participate

Not applicable.

### Consent for publication

Not applicable.

### Copyright

© The Author(s) 2025.

## REFERENCES

1. Scott, J. F.; Paz, A. C. A. Ferroelectric memories. *Science* **1989**, *246*, 1400-5. DOI PubMed
2. Kang, S.; Jang, W. S.; Morozovska, A. N.; et al. Highly enhanced ferroelectricity in  $HfO_2$ -based ferroelectric thin film by light ion

- bombardment. *Science* **2022**, *376*, 731-8. DOI
3. Park, M. H.; Lee, Y. H.; Kim, H. J.; et al. Ferroelectricity and antiferroelectricity of doped thin HfO<sub>2</sub>-based films. *Adv. Mater.* **2015**, *27*, 1811-31. DOI
  4. Polakowski, P.; Müller, J. Ferroelectricity in undoped hafnium oxide. *Appl. Phys. Lett.* **2015**, *106*, 232905. DOI
  5. Müller, J.; Böske, T. S.; Müller, S.; et al. Ferroelectric hafnium oxide: a CMOS-compatible and highly scalable approach to future ferroelectric memories. In Proceedings of the 2013 IEEE International Electron Devices Meeting; 9-11 December 2013, Washington, DC, USA. DOI
  6. Böske, T. S.; Müller, J.; Bräuhäus, D.; Schröder, U.; Böttger, U. Ferroelectricity in hafnium oxide thin films. *Appl. Phys. Lett.* **2011**, *99*, 102903. DOI
  7. Mikolajick, T.; Slesazek, S.; Park, M. H.; Schroeder, U. Ferroelectric hafnium oxide for ferroelectric random-access memories and ferroelectric field-effect transistors. *MRS. Bull.* **2018**, *43*, 340-6. DOI
  8. Sang, X.; Grimley, E. D.; Schenk, T.; Schroeder, U.; Lebeau, J. M. On the structural origins of ferroelectricity in HfO<sub>2</sub> thin films. *Appl. Phys. Lett.* **2015**, *106*, 162905. DOI
  9. Jia, Y.; Yang, Q.; Fang, Y. W.; et al. Giant tunnelling electroresistance in atomic-scale ferroelectric tunnel junctions. *Nat. Commun.* **2024**, *15*, 693. DOI PubMed PMC
  10. Hao, Y.; Chen, X.; Zhang, L.; et al. Record high room temperature resistance switching in ferroelectric-gated Mott transistors unlocked by interfacial charge engineering. *Nat. Commun.* **2023**, *14*, 8247. DOI PubMed PMC
  11. Lee, T. Y.; Lee, K.; Lim, H. H.; et al. Ferroelectric polarization-switching dynamics and wake-up effect in Si-doped HfO<sub>2</sub>. *ACS. Appl. Mater. Interfaces.* **2019**, *11*, 3142-9. DOI
  12. Grimley, E. D.; Schenk, T.; Mikolajick, T.; Schroeder, U.; Lebeau, J. M. Atomic structure of domain and interphase boundaries in ferroelectric HfO<sub>2</sub>. *Adv. Mater. Inter.* **2018**, *5*, 1701258. DOI
  13. Batra, R.; Huan, T. D.; Jones, J. L.; Rossetti, G.; Ramprasad, R. Factors favoring ferroelectricity in hafnia: a first-principles computational study. *J. Phys. Chem. C.* **2017**, *121*, 4139-45. DOI
  14. Schroeder, U.; Park, M. H.; Mikolajick, T.; Hwang, C. S. The fundamentals and applications of ferroelectric HfO<sub>2</sub>. *Nat. Rev. Mater.* **2022**, *7*, 653-69. DOI
  15. Mittmann, T.; Materano, M.; Chang, S. C.; Karpov, I.; Mikolajick, T.; Schroeder, U. Impact of Oxygen Vacancy Content in Ferroelectric HZO films on the Device Performance. In Proceedings of the 2020 IEEE International Electron Devices Meeting (IEDM); 12-18 December 2020, San Francisco, CA, USA. DOI
  16. He, R.; Wu, H.; Liu, S.; Liu, H.; Zhong, Z. Ferroelectric structural transition in hafnium oxide induced by charged oxygen vacancies. *Phys. Rev. B.* **2021**, *104*, L180102. DOI
  17. Zhou, Y.; Zhang, Y.; Yang, Q.; et al. The effects of oxygen vacancies on ferroelectric phase transition of HfO<sub>2</sub>-based thin film from first-principle. *Comput. Mater. Sci.* **2019**, *167*, 143-50. DOI
  18. Muñoz Ramo, D.; Shluger, A. L.; Gavartin, J. L.; Bersuker, G. Theoretical prediction of intrinsic self-trapping of electrons and holes in monoclinic HfO<sub>2</sub>. *Phys. Rev. Lett.* **2007**, *99*, 155504. DOI PubMed
  19. Yan, F.; Wu, Y.; Liu, Y.; et al. Recent progress on defect-engineering in ferroelectric HfO<sub>2</sub>: the next step forward via multiscale structural optimization. *Mater. Horiz.* **2024**, *11*, 626-45. DOI
  20. Shao, M.; Liu, H.; He, R.; et al. Programmable ferroelectricity in Hf<sub>0.5</sub>Zr<sub>0.5</sub>O<sub>2</sub> enabled by oxygen defect engineering. *Nano. Lett.* **2024**, *24*, 1231-7. DOI
  21. Lee, J.; Yang, K.; Kwon, J. Y.; et al. Role of oxygen vacancies in ferroelectric or resistive switching hafnium oxide. *Nano. Converg.* **2023**, *10*, 55. DOI PubMed PMC
  22. Materano, M.; Mittmann, T.; Lomenzo, P. D.; et al. Influence of oxygen content on the structure and reliability of ferroelectric Hf<sub>x</sub>Zr<sub>1-x</sub>O<sub>2</sub> layers. *ACS. Appl. Electron. Mater.* **2020**, *2*, 3618-26. DOI
  23. Bao, K.; Liao, J.; Yan, F.; et al. Enhanced endurance and imprint properties in Hf<sub>0.5</sub>Zr<sub>0.5</sub>O<sub>2-δ</sub> ferroelectric capacitors by tailoring the oxygen vacancy. *ACS. Appl. Electron. Mater.* **2023**, *5*, 4615-23. DOI
  24. Zheng, Y.; Zhang, Y.; Xin, T.; et al. Direct atomic-scale visualization of the 90° domain walls and their migrations in Hf<sub>0.5</sub>Zr<sub>0.5</sub>O<sub>2</sub> ferroelectric thin films. *Mater. Today. Nano.* **2023**, *24*, 100406. DOI
  25. Bai, F.; Liao, J.; Yang, J.; et al. Mechanical-electrical-chemical coupling study on the stabilization of a hafnia-based ferroelectric phase. *NPJ. Comput. Mater.* **2023**, *9*, 1176. DOI
  26. Fan, P.; Zhang, Y. K.; Yang, Q.; et al. Origin of the intrinsic ferroelectricity of HfO<sub>2</sub> from ab initio molecular dynamics. *J. Phys. Chem. C.* **2019**, *123*, 21743-50. DOI
  27. Dogan, M.; Gong, N.; Ma, T. P.; Ismail-Beigi, S. Causes of ferroelectricity in HfO<sub>2</sub>-based thin films: an ab initio perspective. *Phys. Chem. Chem. Phys.* **2019**, *21*, 12150-62. DOI
  28. Shiraiishi, T.; Katayama, K.; Yokouchi, T.; et al. Impact of mechanical stress on ferroelectricity in (Hf<sub>0.5</sub>Zr<sub>0.5</sub>)O<sub>2</sub> thin films. *Appl. Phys. Lett.* **2016**, *108*, 262904. DOI
  29. Bouaziz, J.; Romeo, P. R.; Baboux, N.; Vilquin, B. Huge reduction of the wake-up effect in ferroelectric HZO thin films. *ACS. Appl. Electron. Mater.* **2019**, *1*, 1740-5. DOI
  30. Luo, Q.; Cheng, Y.; Yang, J.; et al. A highly CMOS compatible hafnia-based ferroelectric diode. *Nat. Commun.* **2020**, *11*, 1391. DOI PubMed PMC
  31. Chen, L.; Liang, Z.; Shao, S.; Huang, Q.; Tang, K.; Huang, R. First direct observation of the built-in electric field and oxygen vacancy

- migration in ferroelectric  $\text{Hf}_{0.5}\text{Zr}_{0.5}\text{O}_2$  film during electrical cycling. *Nanoscale* **2023**, *15*, 7014-22. DOI
32. Hanson, E. D.; Lajaunie, L.; Hao, S.; et al. Systematic study of oxygen vacancy tunable transport properties of few-layer  $\text{MoO}_{3-x}$  enabled by vapor-based synthesis. *Adv. Funct. Mater.* **2017**, *27*, 1605380. DOI
  33. Bhat, J.; Maddani, K.; Karguppikar, A.; Ganesh, S. Electron beam radiation effects on electrical and optical properties of pure and aluminum doped tin oxide films. *Nucl. Instrum. Meth. Phys. Res. B.* **2007**, *258*, 369-74. DOI
  34. Barzilay, M.; Qiu, T.; Rappe, A. M.; Ivry, Y. Epitaxial  $\text{TiO}_x$  surface in ferroelectric  $\text{BaTiO}_3$ ; native structure and dynamic patterning at the atomic scale. *Adv. Funct. Mater.* **2020**, *30*, 1902549. DOI
  35. Vogel, T.; Kaiser, N.; Petzold, S.; et al. Defect-induced phase transition in hafnium oxide thin films: comparing heavy ion irradiation and oxygen-engineering effects. *IEEE. Trans. Nucl. Sci.* **2021**, *68*, 1542-7. DOI
  36. Zheng, Y.; Zhong, C.; Zheng, Y.; et al. In-situ atomic visualization of structural transformation in  $\text{Hf}_{0.5}\text{Zr}_{0.5}\text{O}_2$  ferroelectric thin film: from nonpolar tetragonal phase to polar orthorhombic phase. In Proceedings of the 2021 Symposium on VLSI Technology; 13-19 June 2021, Kyoto, Japan. Available from: <https://ieeexplore.ieee.org/document/9508736> [Last accessed on 14 Mar 2025].
  37. Ma, L. Y.; Liu, S. Structural polymorphism kinetics promoted by charged oxygen vacancies in  $\text{HfO}_2$ . *Phys. Rev. Lett.* **2023**, *130*, 096801. DOI
  38. Liu, S.; Hanrahan, B. M. Effects of growth orientations and epitaxial strains on phase stability of  $\text{HfO}_2$  thin films. *Phys. Rev. Mater.* **2019**, *3*, 054404. DOI
  39. Xin, T.; Zheng, Y.; Cheng, Y.; et al. Atomic visualization of the emergence of orthorhombic phase in  $\text{Hf}_{0.5}\text{Zr}_{0.5}\text{O}_2$  ferroelectric film with in-situ rapid thermal annealing. In Proceedings of the 2022 IEEE Symposium on VLSI Technology and Circuits (VLSI Technology and Circuits); 12-17 June 2022, Honolulu, HI, USA. DOI
  40. Grimley, E. D.; Schenk, T.; Sang, X.; et al. Structural changes underlying field-cycling phenomena in ferroelectric  $\text{HfO}_2$  thin films. *Adv. Elect. Mater.* **2016**, *2*, 1600173. DOI
  41. Han, R.; Hong, P.; Ning, S.; et al. The effect of stress on  $\text{HfO}_2$ -based ferroelectric thin films: a review of recent advances. *J. Appl. Phys.* **2023**, *133*, 240702. DOI
  42. Saini, B.; Huang, F.; Choi, Y.; et al. Field-induced ferroelectric phase evolution during polarization “wake-up” in  $\text{Hf}_{0.5}\text{Zr}_{0.5}\text{O}_2$  thin film capacitors. *Adv. Elect. Mater.* **2023**, *9*, 2300016. DOI
  43. Pešić, M.; Fengler, F. P. G.; Larcher, L.; et al. Physical mechanisms behind the field-cycling behavior of  $\text{HfO}_2$ -based ferroelectric capacitors. *Adv. Funct. Mater.* **2016**, *26*, 4601-12. DOI
  44. Yang, J.; Liao, J.; Huang, J.; Yan, F.; Liao, M.; Zhou, Y. Kinetic phase transition paths and phase stability in ferroelectric  $\text{HfO}_2$ . *Scripta. Mater.* **2024**, *242*, 115953. DOI
  45. Inenaga, K.; Motomura, R.; Ishimaru, M.; Nakamura, R.; Yasuda, H. Liquid-mediated crystallization of amorphous GeSn under electron beam irradiation. *J. Appl. Phys.* **2020**, *127*, 205304. DOI
  46. Yin, X.; Müller, F.; Huang, Q.; et al. An ultracompact single-ferroelectric field-effect transistor binary and multibit associative search engine. *Adv. Intell. Syst.* **2023**, *5*, 2200428. DOI
  47. Zheng, Y.; Zheng, Y.; Gao, Z.; et al. Atomic-scale characterization of defects generation during fatigue in ferroelectric  $\text{Hf}_{0.5}\text{Zr}_{0.5}\text{O}_2$  films: vacancy generation and lattice dislocation. In Proceedings of the 2021 IEEE International Electron Devices Meeting (IEDM); 11-16 December 2021, San Francisco, CA, USA. DOI